

NACA RM L52E06a



NACA

RESEARCH MEMORANDUM

FLUTTER OF A 60° DELTA WING (NACA 65A003 AIRFOIL)

ENCOUNTERED AT SUPERSONIC SPEEDS DURING THE

FLIGHT TEST OF A ROCKET-PROPELLED MODEL

By Joseph H. Judd and William T. Lauten, Jr.

Langley Aeronautical Laboratory
Langley Field, Va.

**NATIONAL ADVISORY COMMITTEE
FOR AERONAUTICS**

WASHINGTON
September 25, 1952

subjection cancelled (or changed to UNCLASSIFIED.....)

authored by WASH TECH PWD ANNUAL REPORT #15
(OFFICER AUTHORIZED TO CHANGE)

E) ..

20 May 57

CHAP

GRADE OF OFFICER MAKING CHANGE)

2 April
DATE



NATIONAL ADVISORY COMMITTEE FOR AERONAUTICS

RESEARCH MEMORANDUM

FLUTTER OF A 60° DELTA WING (NACA 65A003 AIRFOIL)

ENCOUNTERED AT SUPERSONIC SPEEDS DURING THE

FLIGHT TEST OF A ROCKET-PROPELLED MODEL

By Joseph H. Judd and William T. Lauten, Jr.

SUMMARY

Flight-test results obtained from a 60° delta-wing (NACA 65A003 airfoil section) airplane configuration indicated wing flutter during latter portion of accelerating flight to the peak Mach number of 2.29 and during decelerating flight to a Mach number of 1.07 without apparent damage to the wing. An abrupt change of the frequency of wing oscillation, occurring at Mach number 1.80, indicated a change in the mode of flutter. The ratio of flutter frequency to the third natural frequency of the wing decreased from 1.0 above a Mach number of 1.80 to approximately 0.62 below a Mach number of 1.72. Similar changes in mode of flutter were observed during wind-tunnel tests of a 45° delta wing having an NACA 16-004 airfoil section. A gradual change in flutter frequency, approximately proportional to the change of air density, occurred during each mode of flutter.

The natural frequencies of vibration of the flight-model wing and the structural influence coefficients of a similar semispan wing and the mass, moment of inertia, and center of gravity of streamwise strips of the semispan wing, as determined from laboratory tests, are presented.

INTRODUCTION

Recent studies have indicated that thin delta wings show promise for supersonic aircraft. While a considerable amount of data on the aerodynamic characteristics of these wings has been obtained over a wide range of Mach numbers, the amount of experimental flutter data on delta wings is small. Some data on supersonic flutter of delta wings are presented in references 1 and 2 and data on subsonic flutter are presented in reference 3.

As part of an investigation of the zero-lift drag of airplane configurations with wing-mounted nacelles, a model having a 60° delta wing (NACA 65A003 airfoil section) was flight-tested without nacelles. During the flight of this configuration a wing vibration, thought to be flutter, occurred during the latter portion of the accelerating flight and continued to the peak Mach number of 2.29 and during decelerating flight to a Mach number of 1.07.

The flutter data obtained during the flight test and the structural characteristics of a wing similar to the flight model are presented in this paper. It is believed that this information will be of use in future design work.

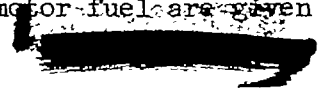
MODEL

A three-view drawing with the model parameters of the flight-model configuration is presented in figure 1. As shown in this figure, a 60° delta wing was located in a high-wing position on the fuselage at zero incidence. Symmetrical aluminum fins of hexagonal airfoil section were mounted vertically on the rear portion of the fuselage. Figure 2 gives two photographs of the model.

The fuselage used in this configuration was a modified transonic body. Fuselage ordinates are presented in table I. The nose of the fuselage was spun from aluminum, while the main fuselage section, on which the wing is mounted, was constructed of laminated mahogany.

The wing used on the flight model had a 60° delta plan form with an NACA 65A003 airfoil section. The airfoil section ordinates at the mean aerodynamic chord are given in table II. A sheet of 0.091-inch aluminum alloy with 0.030-inch maple veneer cycle-welded on each side comprised the core. Mahogany blocks, laid parallel to the wing leading edge, were glued to the core and cut to form the airfoil. The entire wing was made in one piece for the flight model. Since dissection of the wing is necessary to determine completely the desired structural data, a duplicate half-wing was constructed similar to the flight-test wing. Because of the high wing location on the flight model, the wing intersections were different on each surface of the wing. The flight-model wing intersections were duplicated on the ground-test wing by mounting blocks.

A 6.25-inch Deacon rocket motor booster was used to propel the flight model to supersonic speeds. The horizontal booster fins, as shown in figure 2(b), were effectively flat-plate airfoil sections with an area of 12.5 square feet. After separation of the model from the booster, a 3.25-inch rocket motor, mounted in the fuselage, was used to propel the model to the peak Mach number. Weight and balance data for the model with and without rocket-motor fuel are given in table III.



INSTRUMENTATION AND MEASUREMENTS

Flight Test

The data from the flight test were obtained by the use of telemeter, radiosonde, Doppler velocimeter radar, tracking radar, and cameras. Normal and longitudinal accelerations of the model were transmitted and recorded by a telemeter system as the model traversed the speed range. Reduction of data from the radar units supplied time histories of velocity and flight path. A survey of atmospheric data for the test was made through radiosonde measurements from an ascending balloon.

The normal accelerometer had a natural frequency of about 76 cycles per second and was damped to about 58 percent of critical damping. The galvanometer element in the recorder had a natural frequency of 100 cycles per second and was damped to 65 percent of critical damping. The telemeter, accelerometer, and galvanometer give a true reproduction of the frequency throughout the range encountered in this test. The amplitude response of the system is estimated to be about 0.13 of the response at zero frequency for an imposed frequency of 145 cycles per second and about 0.65 at a frequency of 85 cycles per second.

Since the model was unsymmetrical, a slight angle of attack was required to trim the model. The envelop of the normal accelerometer record was read and the mean taken as the value of normal acceleration caused by deviation from the zero-lift flight path. Over a Mach number range of 1.08 to 1.55 the normal-force coefficient increased from 0.005 to 0.0085. Above Mach number 1.55, the normal-force coefficient approached a value of zero. The smallness of these values of normal force indicates that the model was very close to zero angle of attack and that the flutter information may be regarded as zero angle-of-attack data.

Ground Tests

Although flutter was not anticipated during the flight test, the natural frequencies of the wing were obtained experimentally by vibrating the wing over a frequency range of 0 to 250 cycles per second. A sketch of the wing showing the nodal lines for the first three modes of vibration and the frequencies for the first four modes of vibration is presented in figure 3. A similar wing was constructed after the flight test for measurement of the mass and stiffness characteristics. While the wing used in the laboratory tests could not be expected to be an exact duplicate of the wings tested in flight, the two wings were built from the same drawings, and the natural frequencies were nearly the same, so quantities measured should be in good agreement for the two wings.

The quantities determined in the laboratory tests were the structural influence coefficients of the wing, the panel masses of the wing associated with the influence coefficients, and the mass, moment of inertia, and center of gravity of streamwise strips of the wing. The values of these properties are given in tables IV, V, and VI. Figure 4 is a sketch of the wing which shows the root restraint, points of load for influence coefficients, streamwise strips, and wing panels whose masses were determined for use with the structural influence coefficients. For the determination of the influence coefficients, the wing was loaded by a series of wires and pulleys, and deflections were measured with dial gages which could be read directly to 10^{-4} inches. As shown in figure 4, the wing-root supports were not the same for upper and lower surfaces; consequently, a reverse loading was tried at several points. The agreement between readings obtained by loading in opposite directions was within the experimental accuracy of the test, and consequently the effect of different root restraint for upper and lower surfaces was considered negligible. The symmetrically placed terms in table IV have been averaged to agree with Maxwell's reciprocity theorem. The moments of inertia of the streamwise strips were determined by use of a bifilar suspension.

RESULTS AND DISCUSSION

An inspection of the telemeter record of the flight test (portions of which are presented in fig. 5) showed oscillations on the normal accelerometer through part of the accelerating and decelerating flight. After separation of the model from the booster, these oscillations were believed to be caused by wing vibration, since previous experience (refs. 4 and 5) has shown that the normal accelerometer will follow wing vibrations. This wing vibration was attributed to flutter instead of buffeting, since the flow over the wing was supersonic during the period of vibration and the wing was at zero angle of attack and very thin. Prior to separation of the model from the booster, however, the accelerometer oscillations could be caused by vibrations of the model-booster combination. Consequently, the isolation of normal-force vibrations due to the model wing becomes questionable. For this reason the flutter speed (speed at which flutter begins) can be determined for decelerating flight only. The time histories of density, velocity, and Mach number are presented in figure 6. From this figure and the telemeter record, the flutter speed was found to be 1120 feet per second and the flutter Mach number 1.07.

The variation of flutter frequency with Mach number is given in figure 7. A shift in vibration frequency indicated that two distinct modes of flutter occurred during the flight test - one mode whose frequency varied between 150 and 132 cycles per second from Mach number 2.29 to 1.80 and another whose frequency varied between 90 and 72.5 cycles per second from Mach number 1.72 to 1.07. Above Mach number 1.80 the

ratio of flutter frequency to the third natural frequency was 1.00; below Mach number 1.72 the ratio was approximately 0.62. Similar changes in mode of flutter and frequency ratio were observed in tests in the Langley 4.5-foot flutter research tunnel of a 45° delta wing having an NACA 16-004 airfoil section (ref. 3). Flight tests of a 60° delta wing having an NACA 65(06)-006.5 airfoil section (ref. 1) resulted in flutter with a ratio of flutter frequency to third natural frequency of 0.74.

During each mode of flutter a continuous change in flutter frequency occurred. Since the trend in frequency was downward during both accelerating and decelerating flight, the change appears due to the decrease in density, and the frequency was found to be approximately proportional to the density.

CONCLUDING REMARKS

An analysis of the flight time history of a rocket-propelled 60° delta-wing airplane configuration indicated wing flutter during the latter portion of accelerating flight to the maximum Mach number of 2.29 and during decelerating flight to a Mach number of 1.07 with no apparent damage to the wing. During flutter a sudden change in wing frequency from 145 to 85 cycles per second at a Mach number of 1.80 indicated a change in the mode of flutter. Similar changes in mode of flutter were observed during wind-tunnel tests of a 45° delta wing. The flutter frequency gradually changed during each mode of flutter as the air density changed.

The natural frequencies of vibration and the structural influence coefficients of the complete semispan wing and the mass, moment of inertia, and center of gravity of streamwise strips of the wing were subsequently determined by laboratory tests. These data are presented so that this combination of wing structural characteristics may be avoided in future designs. The data may also be useful in a flutter analysis of delta wings.

Langley Aeronautical Laboratory
National Advisory Committee for Aeronautics
Langley Field, Va.

REFERENCES

1. Lauten, William T., Jr., and Mitcham, Grady L.: Note on Flutter of a 60° Delta Wing Encountered at Low-Supersonic Speeds During the Flight of a Rocket-Propelled Model. NACA RM L51B28, 1951.
2. Tuovila, W. J.: Some Wind-Tunnel Results of an Investigation of the Flutter of Sweptback- and Triangular-Wing Models at Mach Number 1.3. NACA RM L52C13, 1952.
3. Herr, Robert W.: A Preliminary Wind-Tunnel Investigation of Flutter Characteristics of Delta Wings. NACA RM L52B14a, 1952.
4. Cunningham, H. J., and Lundstrom, R. R.: Description and Analysis of a Rocket-Vehicle Experiment on Flutter Involving Wing Deformation and Body Motions. NACA RM L50I29, 1950.
5. Lauten, William T., Jr., and Nelson, Herbert C.: Results of Two Free-Fall Experiments on Flutter of Thin Unswept Wings in the Transonic Speed Range. NACA RM L51C08, 1951.

TABLE I

FUSELAGE ORDINATES

Axial distance measured from nose (in.)	Radius (in.)
0	0
.4	.185
.6	.235
1.0	.342
2.0	.578
4.0	.964
6.0	1.290
8.0	1.577
12.0	2.074
16.0	2.472
20.0	2.772
24.0	2.993
28.0	3.146
32.0	3.250
36.0	3.314
40.0	3.334
44.0	3.304
48.0	3.219
52.0	3.037
56.0	2.849
60.0	2.661
64.0	2.474
66.7	2.347



TABLE II

AIRFOIL ORDINATES AT THE MEAN

AERODYNAMIC CHORD

Chordwise distance from leading edge (in.)	Vertical displacement from mean chord line (in.)
0	0
.108	.050
.162	.061
.270	.077
.540	.106
1.080	.142
1.620	.172
2.160	.193
3.240	.236
4.320	.267
5.400	.290
6.480	.306
7.560	.318
8.640	.323
9.710	.323
10.800	.316
11.880	.301
12.970	.280
14.040	.255
15.120	.226
16.200	.192
17.280	.155
18.490	.117
19.400	.079
20.500	.046
21.600	.007


 NACA

TABLE III

WEIGHT AND BALANCE DATA FOR FLIGHT MODEL

Model with rocket fuel:

Weight, lb	71.60
Wing loading, lb/sq ft	17.01
Center-of-gravity position, percent M.A.C.	-14.8

Model without rocket fuel:

Weight, lb	61.75
Wing loading, lb/sq ft	14.68
Center-of-gravity position, percent M.A.C.	-16.2



[]

TABLE IV

STRUCTURAL INFLUENCE COEFFICIENTS

[15-pound load; deflections are in 10^{-4} inches]

Load at station Deflection at station	1	2	3	4	5	6	7	8	9	10	11	12	13
1	41	17	36	5	16	32	2	4	16	26	24	39	26
2	17	34	50	17	43	72	11	30	59	86	67	99	83
3	36	50	180	38	118	220	17	75	159	251	186	272	229
4	5	17	38	48	66	90	40	84	119	148	102	127	150
5	16	43	118	66	174	290	49	177	321	457	312	436	457
6	32	72	220	90	290	768	66	275	585	967	614	968	930
7	2	11	17	40	49	66	145	168	156	141	99	109	173
8	4	30	75	84	177	257	168	420	501	564	369	473	690
9	16	59	159	119	321	585	156	501	1000	1427	781	1192	1625
10	26	86	251	148	457	967	141	564	1427	2770	1194	2238	2886
11	24	67	186	102	312	614	99	369	781	1194	696	1100	1205
12	39	99	272	127	436	968	109	473	1192	2238	1100	2066	2234
13	26	83	229	150	457	930	173	690	1625	2886	1205	2234	3491

NACA

TABLE V
MASS OF NUMBERED PANELS OF WING
SHOWN IN FIGURE 4

Panel designation (see fig. 4)	Mass (slugs)
01	0.000907
02	.000704
03	.000684
04	.000482
1	.000941
2	.001209
3	.000884
4	.001048
5	.000969
6	.000541
7	.000629
8	.000616
9	.000407
10	.0002052
11	.000404
12	.000202
13	.0001473



TABLE VI
 PROPERTIES OF STREAMWISE STRIPS OF WING SHOWN IN FIGURE 4

Streamwise strips	Spanwise station (inches from wing tip)	Center of gravity		Mass (slugs)	Mass polar moment of inertia (in.-lb-sec ²)
		Inches from tip (spanwise)	Inches from trailing edge (chordwise)		
I	0.0 to 4.8	3.40	3.20	0.00568	0.001794
II	4.8 to 8.0	6.60	6.20	.01368	.01162
III	8.0 to 11.2	9.70	9.10	.02490	.04283
IV	11.2 to 14.4	12.85	12.05	.03855	.1058
V	14.4 to 17.0	15.28	13.10	.03100	.1255

NACA

CONFIDENTIAL

NACA RM 152306a

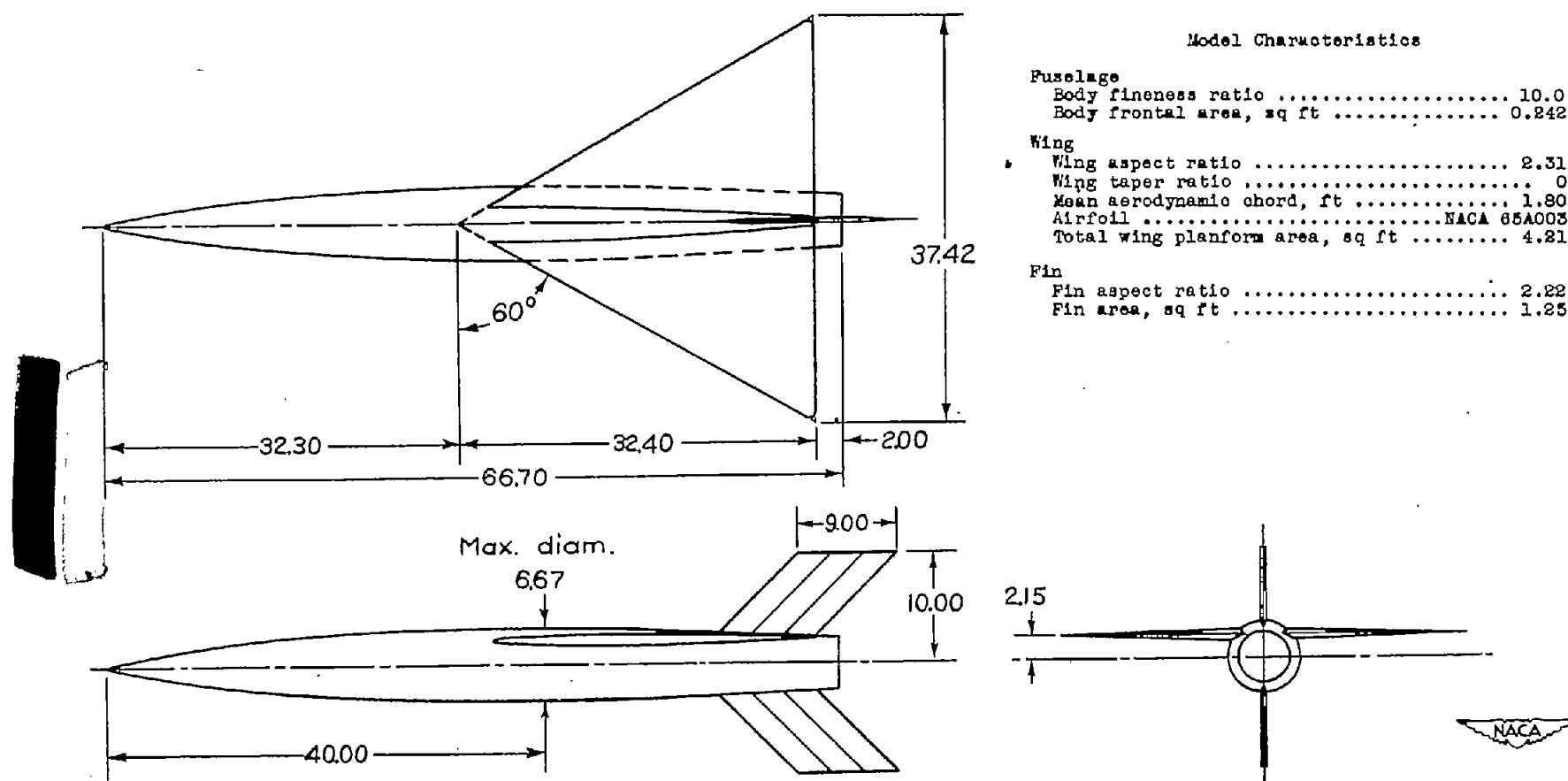
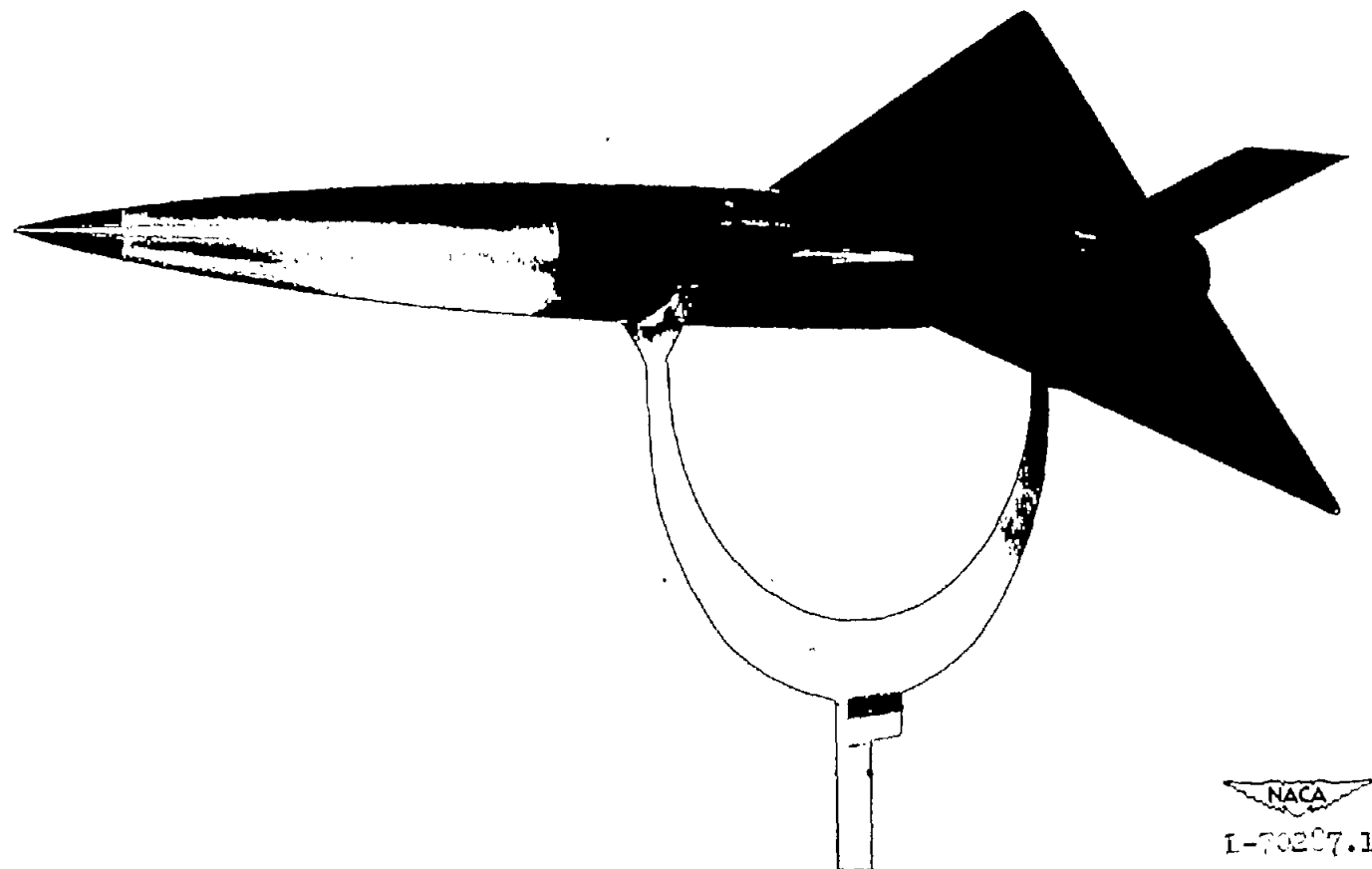


Figure 1.- Three-view drawing of the rocket-powered flight model.
All dimensions in inches.



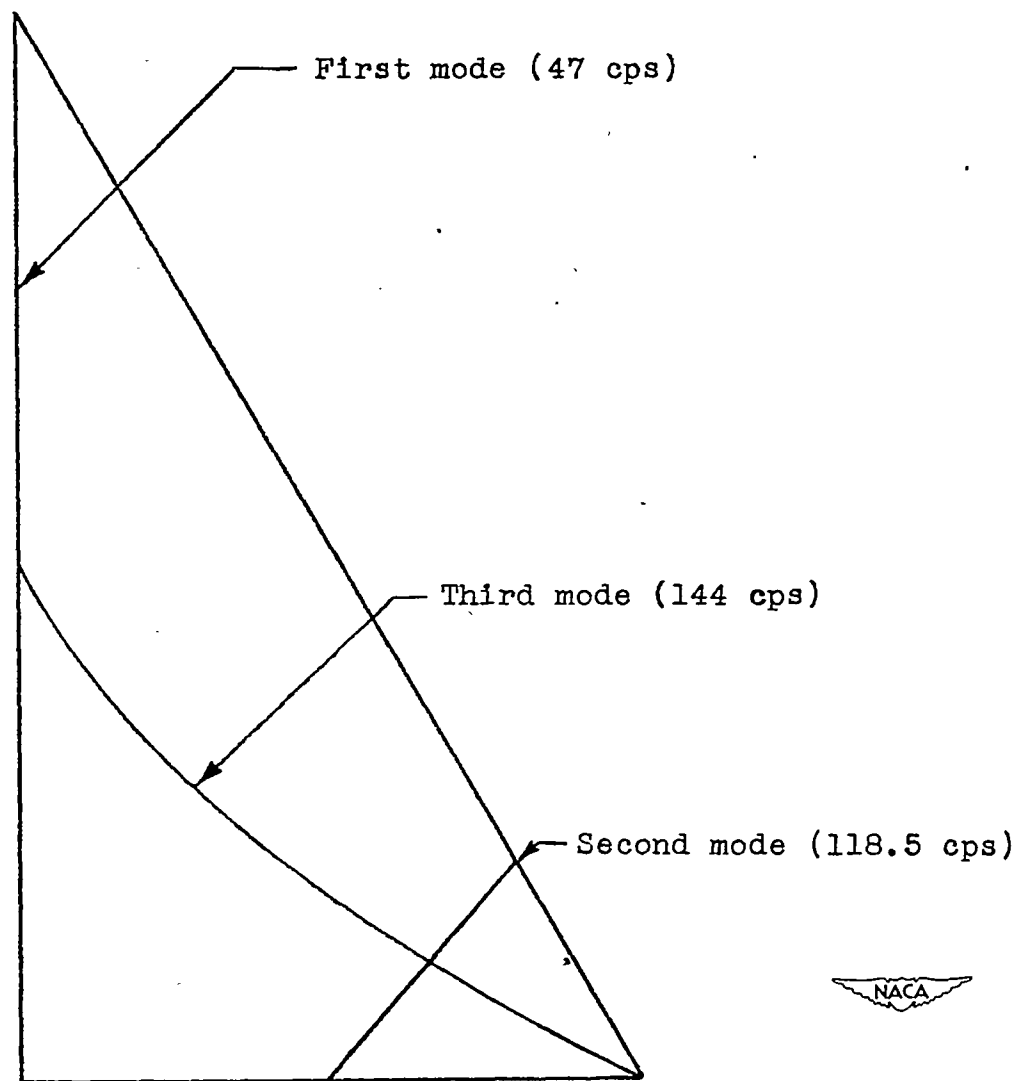
(a) Three-quarter front view of model.

Figure 2.- Photographs of the flight model.



(b) Model and booster on mobile launcher.

Figure 2.- Concluded.



Fourth mode (195 cps)

Figure 3.- Sketch of flight-test wing showing modes of vibration.

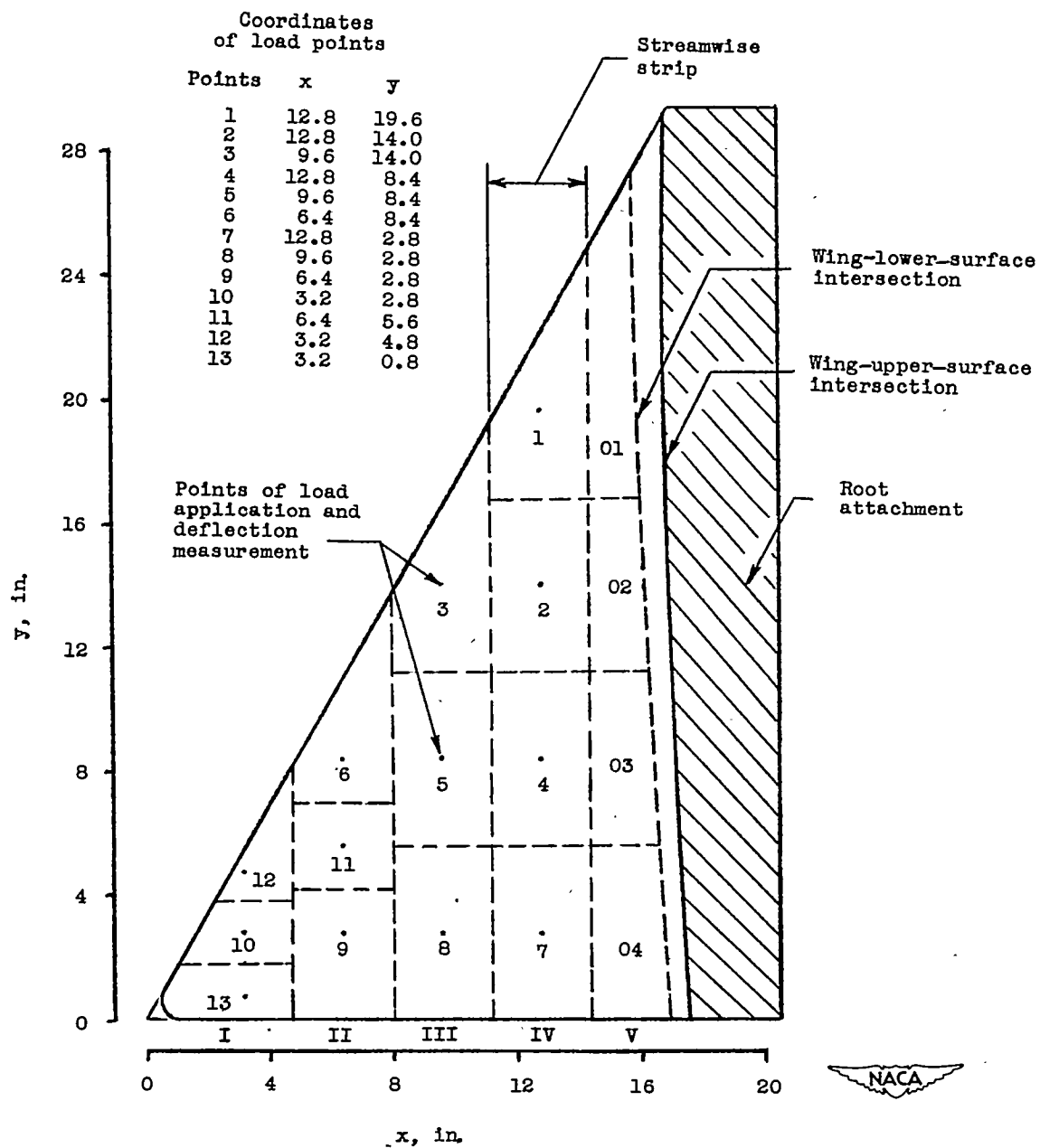
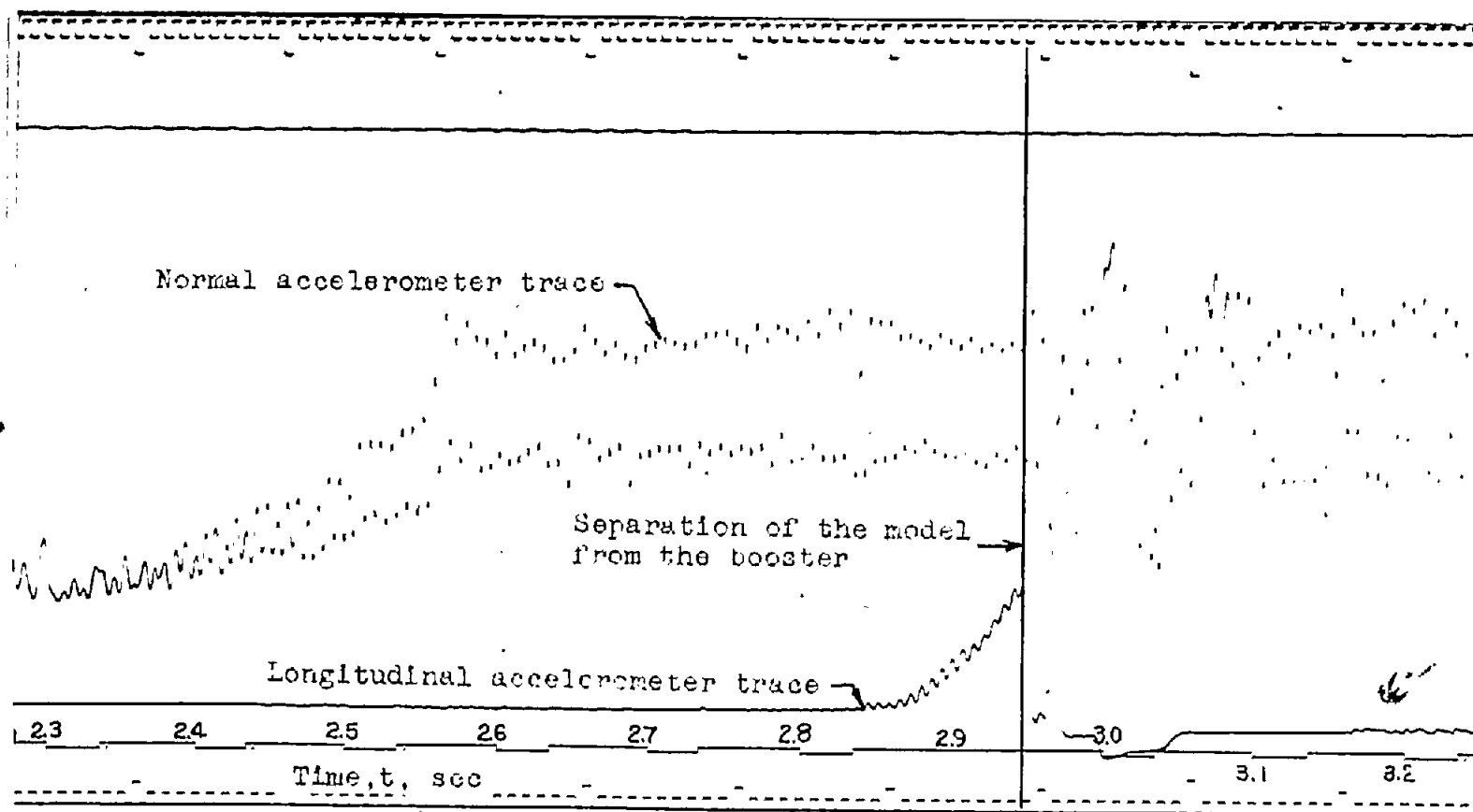


Figure 4.- Schematic drawing of ground-test wing showing unsymmetrical root.

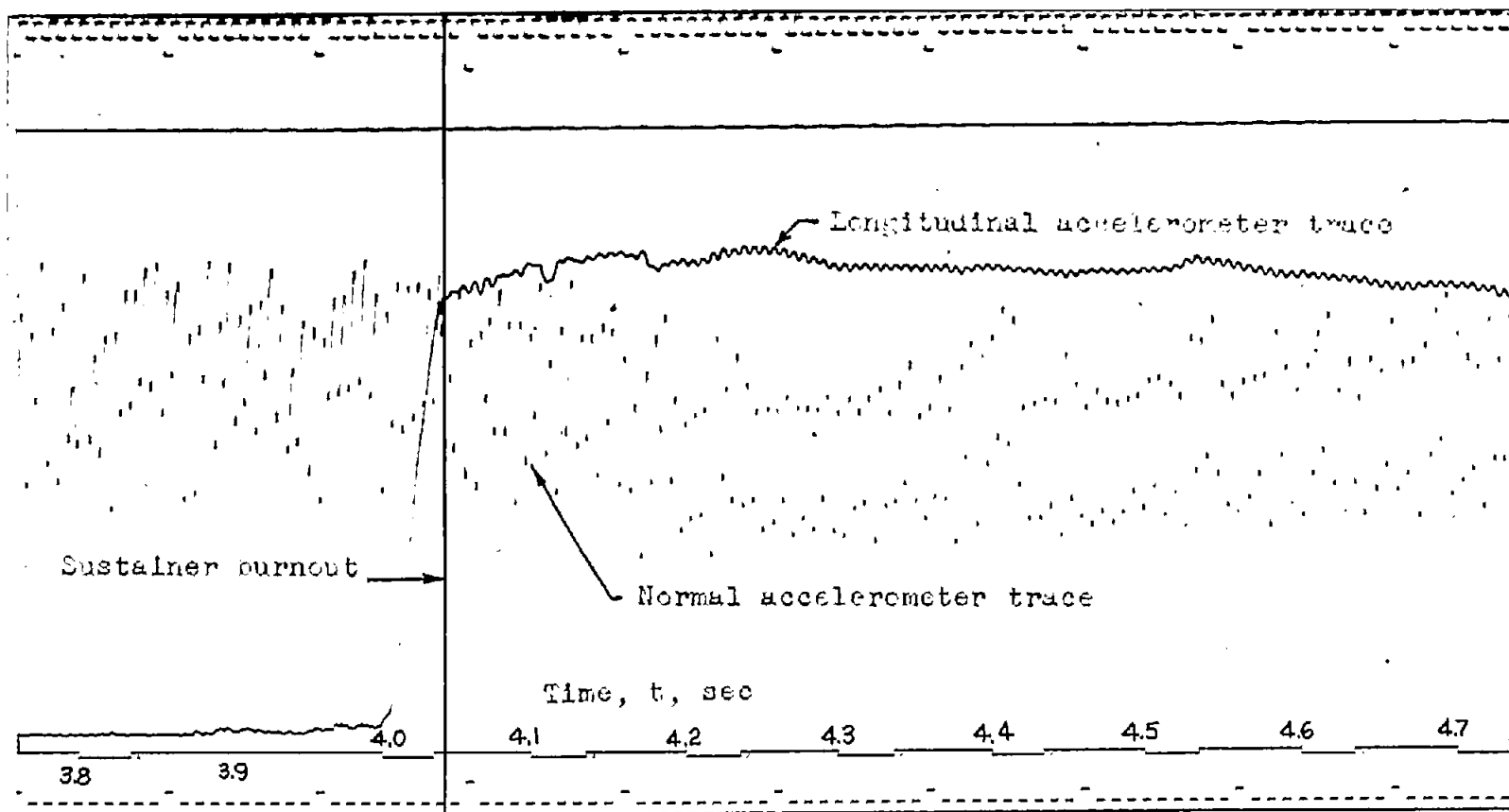


(a) Accelerating flight.

Figure 5.- Portions of the telemeter record.

CONFIDENTIAL

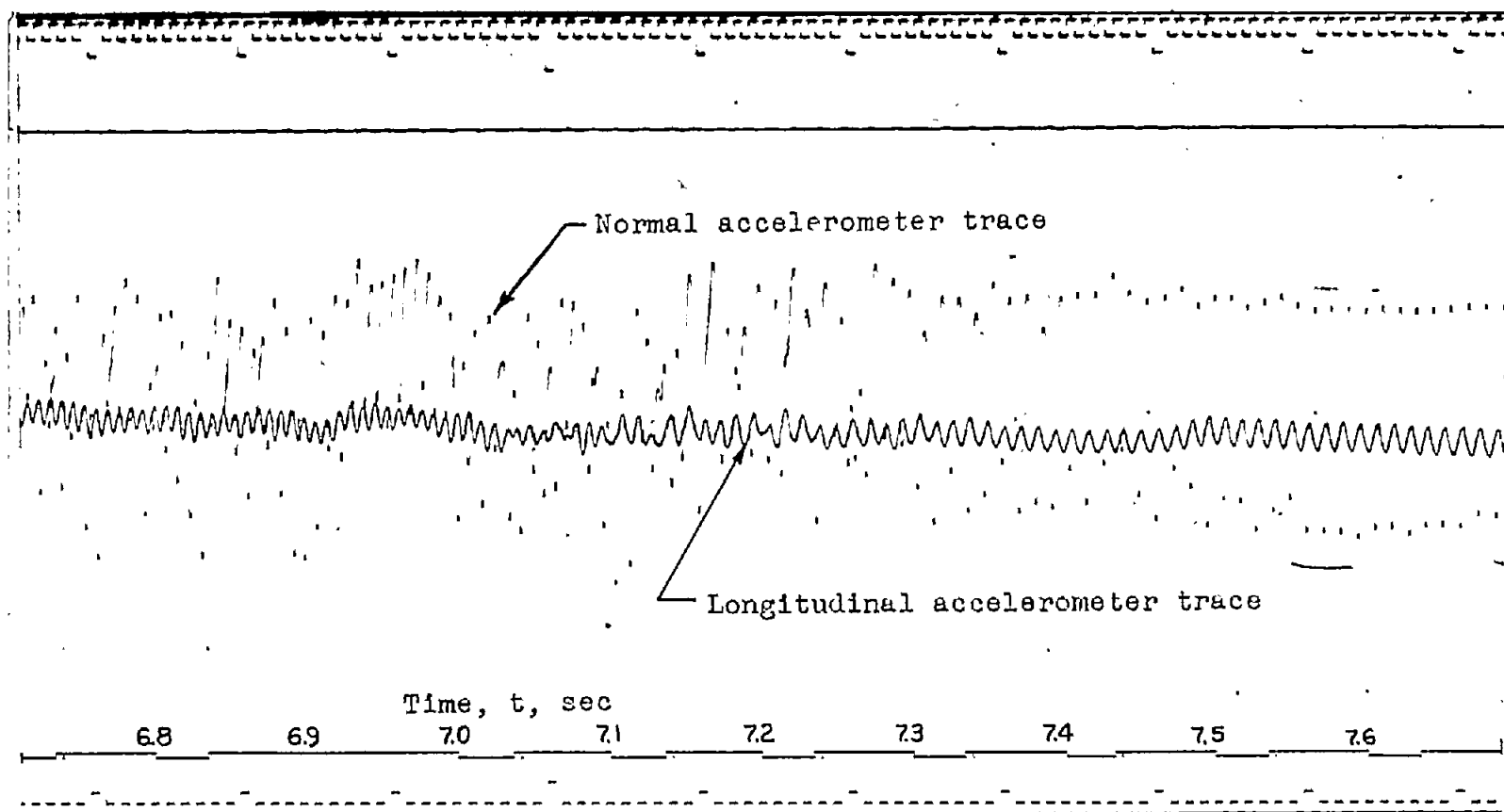
NACA RM L52E06a



(b) Transition from accelerating to decelerating flight.



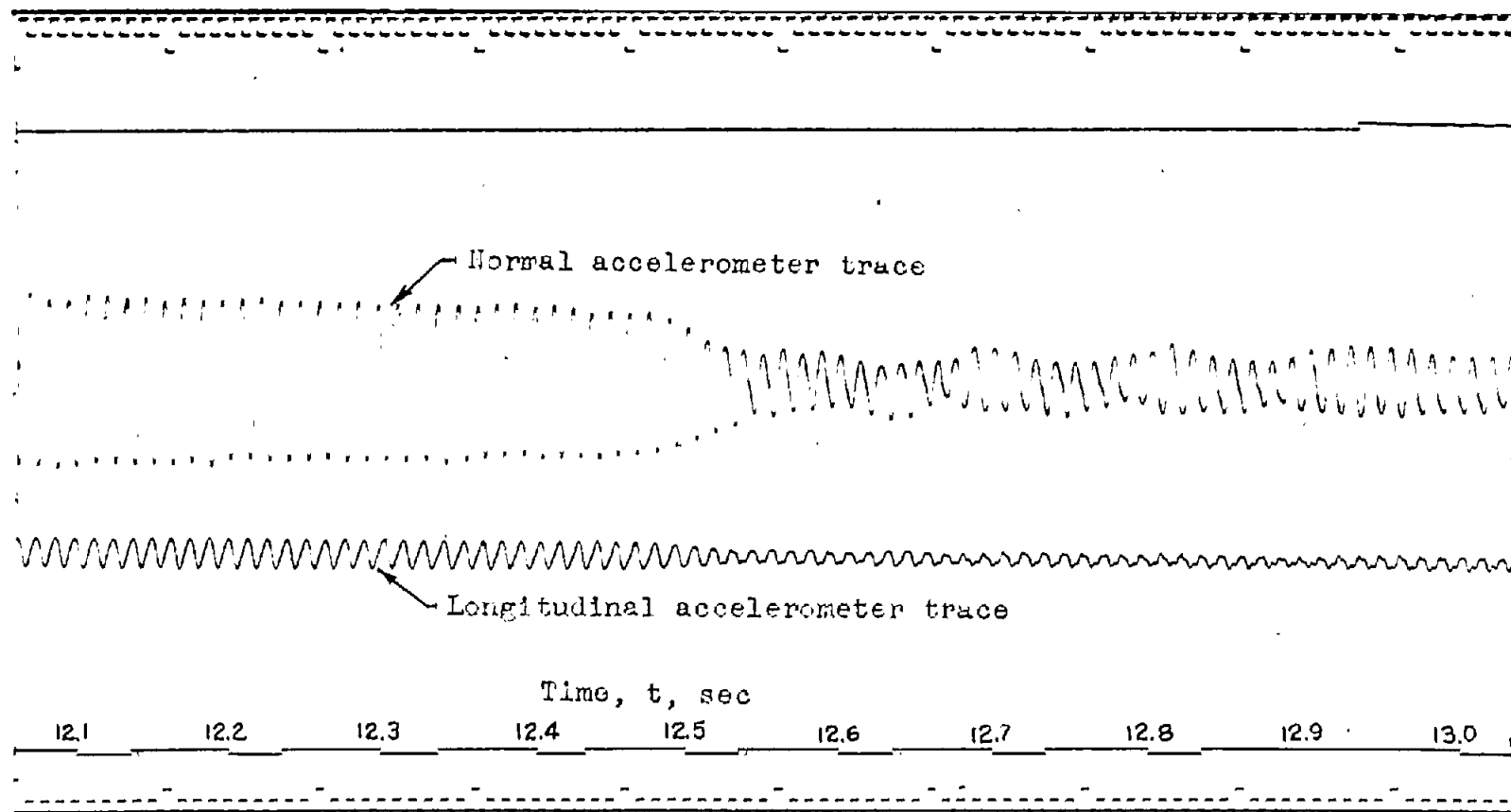
Figure 5.- Continued.



(c) Change in vibration frequency.

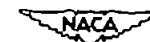
Figure 5.- Continued.

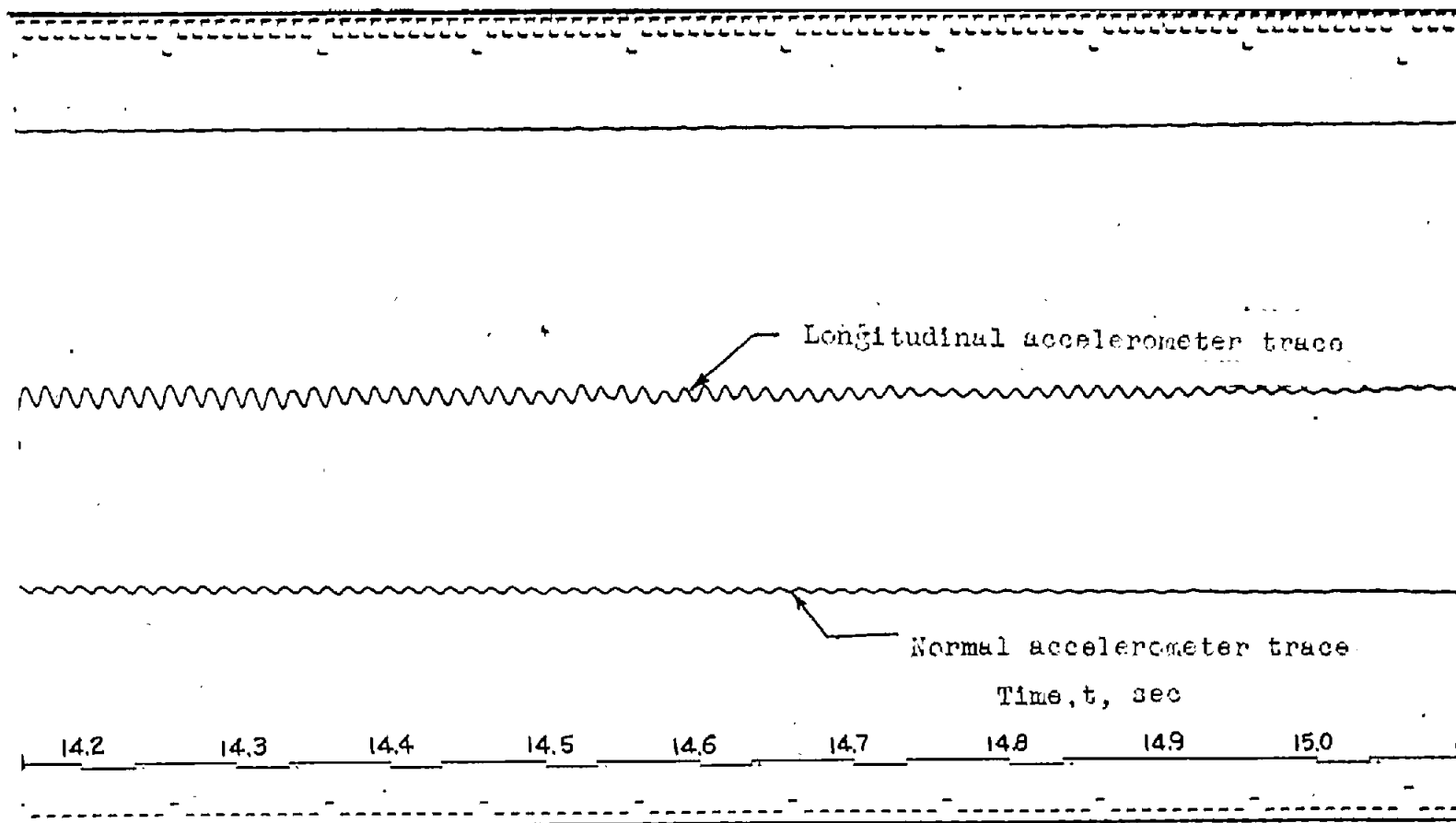




(d) Change in vibration amplitude.

Figure 5.- Continued.





(e) End of vibration.

Figure 5.- Concluded.



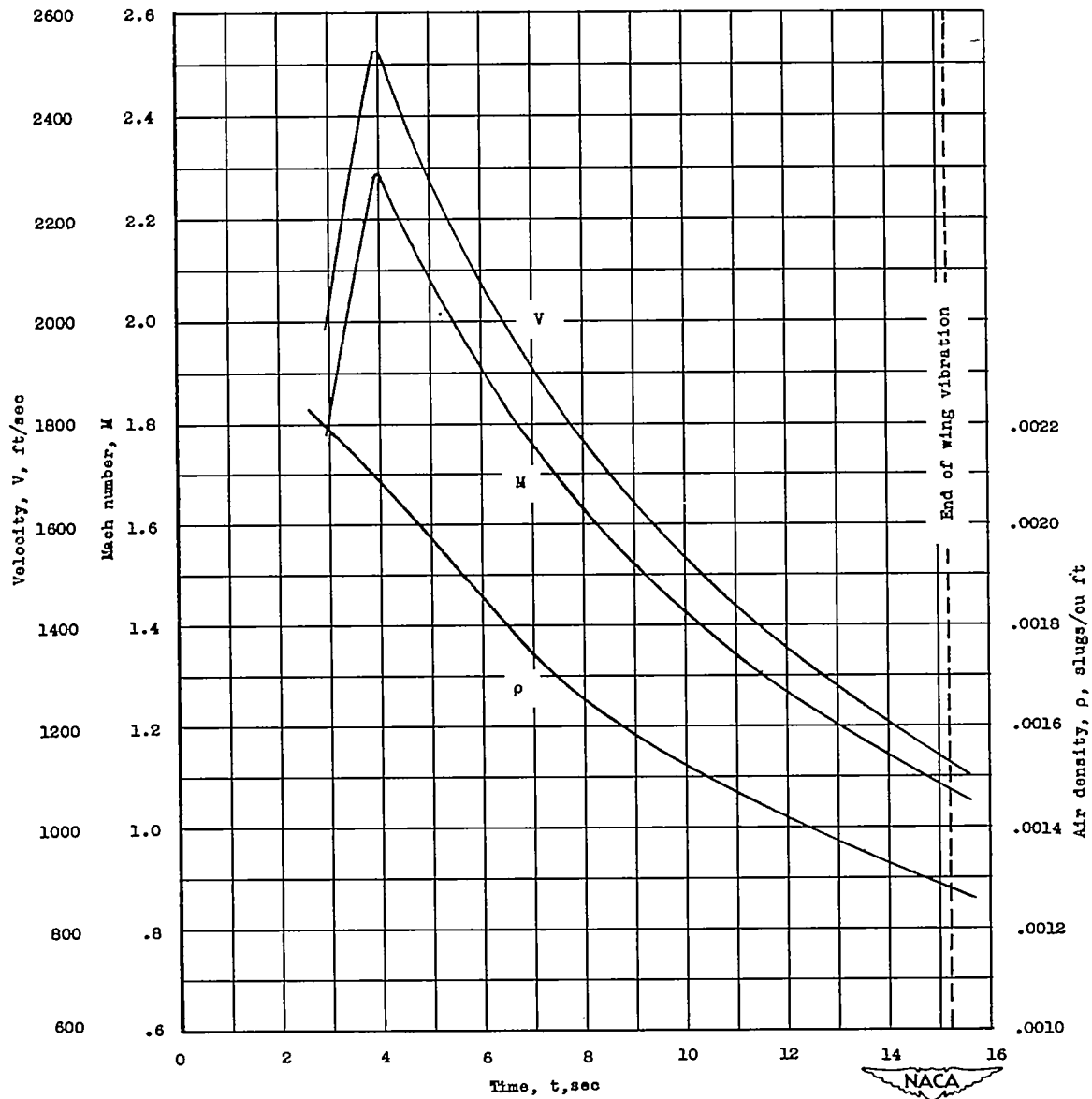


Figure 6.- Variation of Mach number, velocity, and density with time for a portion of the rocket-model flight.

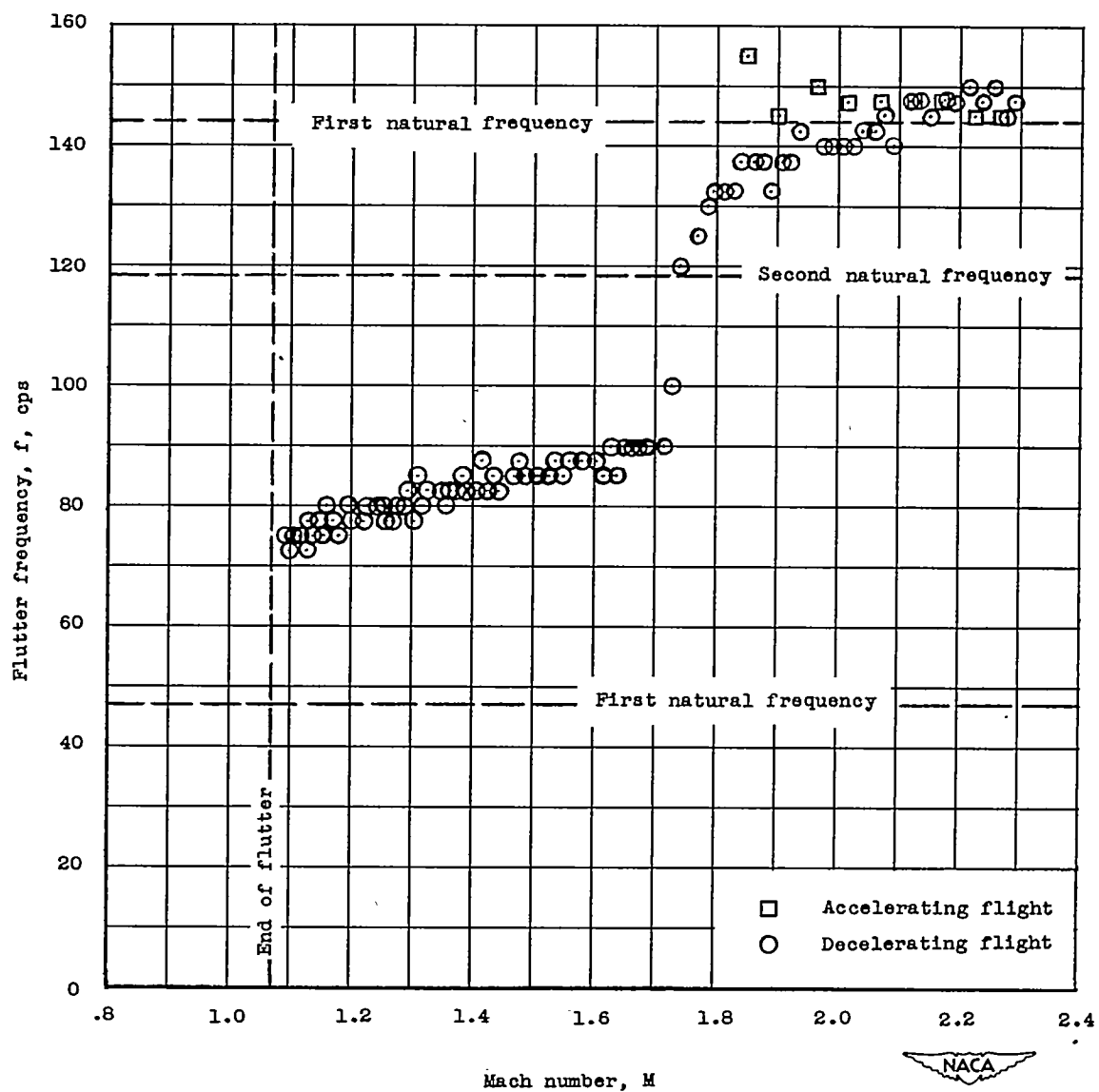


Figure 7.- Variation of flutter frequency with Mach number.